International Journal of Design & Nature and Ecodynamics
Vol. 20, No. 6, June, 2025, pp. 1213-1221
Journal homepage: http://iieta.org/journals/ijdne

Enhanced Cu (II) Removal by Iron-Graphite Electrocoagulation: Kinetics, Efficiency and Hydrogen Co-Production

Amjed Sabah Kamil Janabi[1,2*], Hayder Mohammed Abdul-Hameed[1]

[1] Departments of Environmental Engineering, College of Engineering, University of Baghdad, Baghdad 10071, Iraq
[2] Republic of Iraq Ministry of Construction and Housing, Municipalities and Public Works, Baghdad 10071, Iraq

Corresponding Author Email: amjad.Sabah2311@coeng.uobaghdad.edu.iq

Copyright: ©2025 The authors. This article is published by IIETA and is licensed under the CC BY 4.0 license (http://creativecommons.org/licenses/by/4.0/).

https://doi.org/10.18280/ijdne.200603

Received: 21 May 2025
Revised: 16 June 2025
Accepted: 23 June 2025
Available online: 30 June 2025

Keywords:
Cu (II), electrocoagulation, iron electrode, graphite, wastewater treatment, hydrogen gas production

ABSTRACT

Electrocoagulation (EC) process is an effective electrochemical method of heavy metal removal in wastewater. The removal of Cu (II) in aqueous solutions using Fe-Gr electrodes was studied in the present study in both batch and continuous modes. This was to determine the efficiency of removal of Cu (II) under different operating conditions, such as current density, pH, and treatment time. The originality of the work is that it uses Fe-Gr electrodes, which have the coagulant effect of iron and the high adsorption capacity of graphite. The electrode performance is better, and the removal efficiency is higher for Cu (II) and hydrogen production. The specific surface area (BET) of graphite electrode is 2.6 (m^2/g). The experimental results showed that the pseudo-second-order model was the best fit to the Cu (II) removal kinetics, where $R^2 = 0.98$, which was higher than that of the first-order model, $R^2 = 0.86$, indicating a strong correlation. Graphite offers high electrical conductivity and chemical stability, which facilitates faster electron movement and improved electrode kinetics. During batch experiments, an applied voltage of 50 V and an inter-electrode distance of 3 cm led to almost total removal of Cu (II) in 25 minutes. A 90% percent removal efficiency with H_2 produced was attained with continuous EC experiments at a flow rate of 0.3 L/min and the weight of sludge 12 g. H_2 gas generation (0.152, 0.244, and 0.366 L/min) respectively. This study emphasizes the prospect of Fe-Gr electrodes in enhancing the electrocoagulation process of wastewater treatment, which is more economical and environmentally friendly in controlling the contamination of heavy metals.

1. INTRODUCTION

The issue of sustainable management of water resources is a major problem in the world today because the supply of water has been surpassed by the demand in most parts. Climate change, urbanization, population growth, and industrialization are some of the factors that make this issue even worse [1]. Some of the heavy metals such as mercury (Hg), cadmium (Cd), nickel (Ni), and lead (Pb) are very toxic even in minute amounts, whereas others such as copper (Cu), manganese (Mn), and zinc (Zn) are useful to humans in small doses but can be harmful at higher levels [2, 3]. The World Health Organization (WHO) has established the acceptable limits of some heavy metals in effluents released to the environment: 0.2 mg/L of cyanide, 1 mg/L of copper, 2 mg/L of zinc, and 2 mg/L of nickel [4]. Whereas Cu (II) is vital in low doses in the normal functioning of living cells, in excess of the recommended doses, it may cause serious health problems such as chronic liver diseases, neurological disorders, and psychiatric disorders. Moreover, chromium Cr (VI). and copper Cu (II) have been found to co-exist in wastewater quite frequently [5, 6]. Wastewater that contains both Cr (VI) and Cu (II) is normally harder to treat compared to wastewater that contains either of the two pollutants. Hence, it is important to develop efficient technologies for removing Cr (VI) and Cu (II) wastewater both to protect the environment and to use them on the industrial level. The physical methods of treating Cr (VI)/Cu (II) wastewater are filtration, adsorption, reverse osmosis, and ion exchange, whereas the chemical ones are chemical precipitation [7-10]. Although these traditional methods are effective, high costs, large amounts of chemicals required, and excess sludge produced have led to research on alternative methods that would eliminate these drawbacks [11]. Of these techniques, electrocoagulation has become an electrochemical process of interest. In electrocoagulation, the weak electric current is used to allow the oxidation and dissolution of the sacrificial metals, which are typically iron anodes immersed in wastewater. This results in the production of hydroxide ions, which react with the metal ions of the dissolved anode. The resultant metal hydroxide complexes deprotonate the charges of the contaminants, resulting in the formation of coagulant complexes that are capable of removing pollutants in the water through adsorption [12, 13].

In electrocoagulation, Fe–Al electrodes improve Cu (II) removal via enhanced redox activity and floc formation, while Fe-graphite increases conductivity but shows lower adsorption and coagulant generation efficiency [12]. Fe–Gr electrodes offer high conductivity, chemical stability, and improved

electron transfer, enhancing electrochemical efficiency and reducing energy consumption in treatment systems [11].

This research will set out to determine the efficiency of the electrocoagulation process using Fe-Gr electrodes in the removal of Cu (II) in aqueous solutions in both batch and continuous mode. It is a study of how the removal efficiency of Cu (II) varies along with hydrogen production with different operational parameters, including current density, pH, and treatment time. The originality of the present work consists in the fact that Fe-Gr electrodes are used, which will allow not only to increase the efficiency of removal but also to enhance the electrode performance due to the combination of coagulant properties of iron with the increased adsorption capacity of graphite. The paper also contrasts the batch and continuous electrocoagulation technology, which provides important information on how the two technologies can be used in real life to treat complex wastewater that has Cu (II).

2. MATERIALS AND METHODS

2.1 Materials

The Cu (II) ions employed in the experiment were obtained in the form of cupric nitrate trihydrate, which was purchased in local markets, Baghdad, Iraq, from the scientific equipment suppliers. Table 1 shows the properties of the heavy metal.

Table 1. The main effects and permission limits of Cu (II)

Property	Cu (II)
Chemical name	Cupric nitrate trihydrate
Phase	solid, bluish crystals, odorless
Molecular formula	Cu $(NO_3)_2.3H_2O$
Molecular weight (g/mol)	241.60 g/mol
Density (g/cm^3)	2.05 g/cm^3
Company	Loba Chemie (INDIA)

Preparation of the wastewater that contains 50 ppm of Cupric nitrate trihydrate ion by diluting 2.94 g of Cupric nitrate trihydrate ion in 20 L of tap water. The composition of the supplied wastewater is provided in Table 2.

Table 2. Characteristics of Cu (II) ion sample

Parameter	Value	Unit
pH	6.32	
TDS	102	mg/L
EC	204	µs/cm
Temp.	17.1	℃

2.2 Analysis

The Cu (II) ions concentration was measured by taking 5 mL samples of the Cu (II) solution in the EC cell at different time points. The concentration of the Cu (II) ions in the samples was measured by Atomic Absorption Spectrophotometry (AAS) with a Shimadzu AA-7000F.

2.3 Equipment

The list of equipment utilized throughout the experimental work is provided in Table 3.

Table 3. Instruments utilized in the experimental procedure

Devices Used	Type	Source
Glass ware	Beakers, conical flasks, volumetric flask	China
Sensitive balance	Sartorius	Swiss
Magnetic stirrer	LMS-1003	Korea
Filter paper	Whatman 7.0 cm	China
DC power supply	WANPTEK, type: NPS605W; 0-50V/5A ranging 10-50 V	China
TDS & EC meter	portable A1, EZDO	China
Peristaltic pump	BT100S, GOLANDER PUMP	USA
pH meter	WTW, Bench model	Germany
Atomic absorption flame spectrophotometer	A-shimadzuaa-7000f	Japan

2.4 Electrocoagulation process

Electrocoagulation (EC) is an electrochemical technique that has a number of important benefits, such as versatility, cost-effectiveness, selectivity, safety, low sludge generation, high removal efficiency, and energy efficiency (Figure 1) [14, 15].

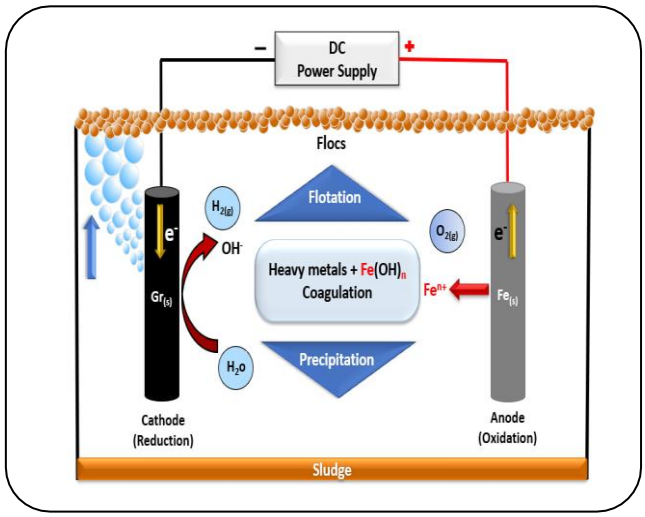

Figure 1. Electrocoagulation schematic diagram

Some of the main operational parameters that affect the electrocoagulation process are inter-electrode distance, pH of the solution, type of electrode, current density, and electrode configuration.

The anodic dissolution reaction (Eq. (1)) forms in-situ coagulants in the electrocoagulation chamber, and hydrogen gas is formed at the cathode (Eq. (2)), and hydroxide ions are formed at the anode (Eq. (3)). These coagulants formed electrochemically are important in the formation of flocs of metal hydroxide that are effective adsorbents in the removal of pollutants [16].

$$\text{At anode: } M(s) \rightarrow M_{aq}^{3+} + ne- \quad (1)$$

$$H_2O \rightarrow 4H_{aq}^{+} + O_2(g) + 4e- \quad (2)$$

At cathode: $nH_2O + ne^- \rightarrow \frac{n}{2} H_2\,(g)\, nOH^-_{aq}$ (3)

2.5 Experimental set-up

The flow chart in Figure 2 shows the experimental procedure of the electrocoagulation process.

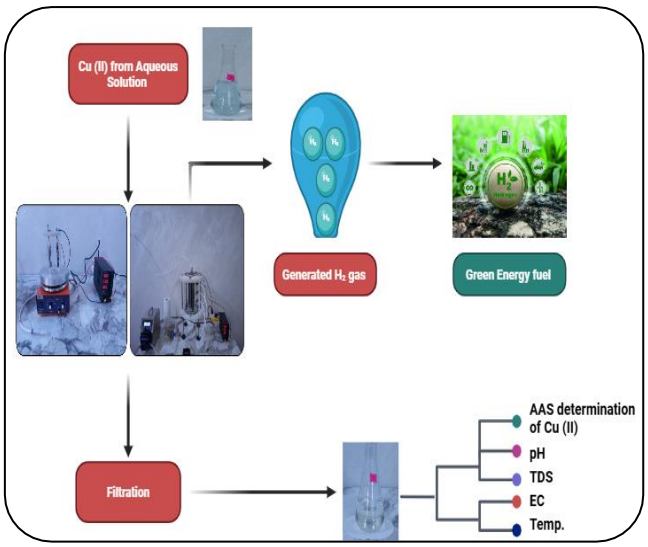

Figure 2. Experimental process in electrocoagulation flow chart

2.6 Batch experiments

The batch experiments were carried out in a 500 mL glass beaker, where 300 mL of heavy metal solution was used, at ambient temperature of 25 +/- 2℃, as depicted in Figure 3. The rectangular shape of iron and graphite electrodes has a length of 9 cm, a width of 3 cm, and a depth of 1cm. Iron was used as an anode and graphite as a cathode in the EC cell.

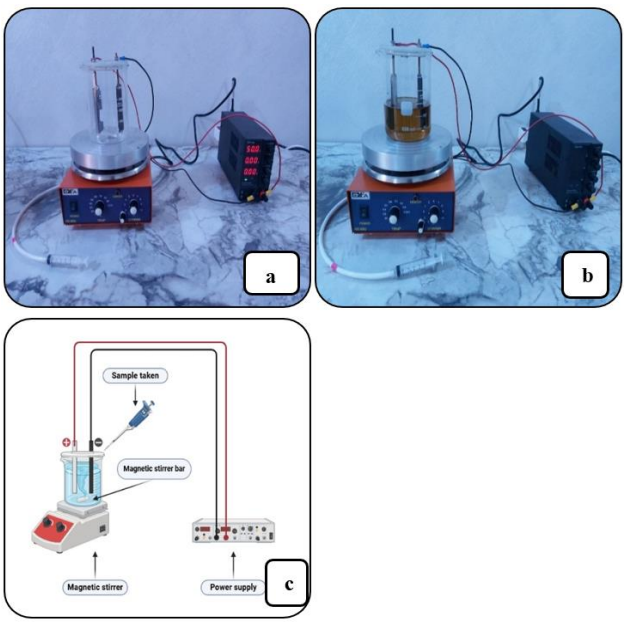

Figure 3. (a) Photographic diagram of batch electrocoagulation instruments with iron anode and graphite cathode, (b) Components and configuration of electrocoagulation instruments used for continuous operation, (c) Schematic diagram of batch electrocoagulation instruments with iron anode and graphite cathode

EC experiments were conducted at various inter-electrode distances ranging from 2, 3, and 4 cm. The electrolyzation time ranged (10, 20, 30, 40, 50, 60, 70, 80, 90) minutes, starting with the DC applied voltage ranging (10, 30, 50) V switching on. Before and after each experiment, pH, TDS, EC, and temperature were measured by a pH meter, TDS, EC, and temperature probe.

The percentage of Cu (II) ion removal was calculated from the following Eq. (4) [17].

$$R(\%) = \frac{(C_o - C_e)}{C_o} \times 100 \quad (4)$$

2.7 Continuous experiments

Aqueous Solution was pumped from the storage feed tank to the reactor, and the flow was controlled by a Peristaltic pump using (0.1, 0.2, 0.3) L/min. Figure 4 shows (a) The system used eight electrodes: four iron anodes and four graphite cathodes, (b) A photo showed the continuous setup with clear electrode placement, (c) Main parts included a reaction cell, power source, and flow system for stable operation, and (d) A schematic explained electrode roles and system configuration. The rectangular shape of iron and graphite electrodes has a length is 22 cm, a width of 3 cm, and a depth of 1cm. Electrodes numbers 4 electrodes iron and 4 electrodes graphite. Iron was used as an anode and graphite as a cathode in the EC reactor. Using voltage from optimum batch experiments: 50 V. During the experiment, the dissolution of ions occurred, and the generation of hydrogen gas was collected in a balloon on the top of the reactor. Different samples were collected every 10 minutes from the port then the current was measured by the clamp meter. Hydrogen gas bubbles are generated as shown in Figure 4; the hydrogen produced is determined and converted to energy and cost revenue when used as a fuel, and the TDS, EC, pH, and temperature inside the reactor are measured. Energy efficiency was 2.7×10^2, 5.66×10^2, 7.60×10^2 KW.

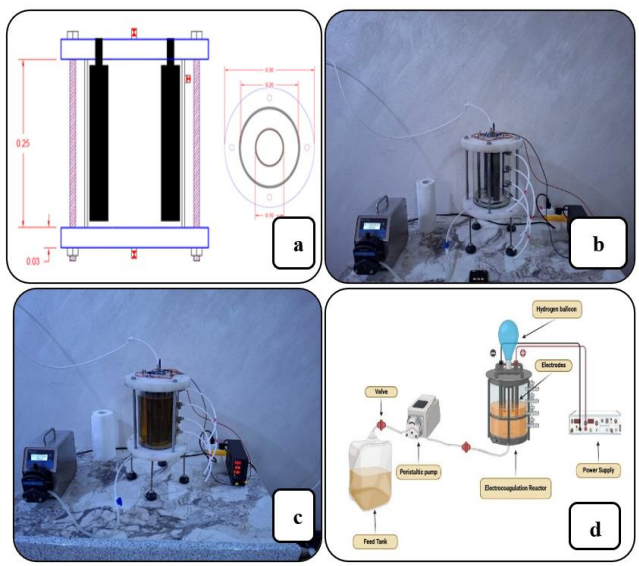

Figure 4. (a) Electrocoagulation set-up (with 8 electrodes: 4 anodes, 4 cathodes), (b) Photographic diagram of continuous electrocoagulation instruments with iron anode and graphite cathode, (c) Components and configuration of electrocoagulation instruments used for continuous operation, (d) Schematic diagram of continuous electrocoagulation instruments with iron anode and graphite cathode

2.8 Kinetics model

The removal kinetics of Cu (II) was examined using two kinetic models: the pseudo-first-order and pseudo-second-order models. These models were applied to experimental data to identify the most suitable one for the system [18, 19]. The analysis was carried out by measuring the rate constants, the equilibrium time, and concentration. The first-order kinetic model can be expressed as follows in general [20]:

$$ln\, C_t = ln\, ct_0 - k_1 \quad (5)$$

Another kinetic model, the second-order model, is also available, and it is especially applicable in systems whose rate-limiting process is the sorption of chemicals [19]. The second-order equation can be written as:

$$\frac{1}{Ct} = k_2 t + \frac{1}{C_{t0}} \quad (6)$$

where, C_0 and Ct are the concentration of Cu (II) at time t = 0 and time t = t, respectively, and k_1 and k_2 are the first- and second-order rate constants. The slopes of the graphs of ln Ct and Ct_1 against t were used to calculate the values of k_1 and k_2 [21].

3. RESULTS AND DISCUSSION

3.1 Batch electrocoagulation results

3.1.1 Removal efficiency at different applied voltage and electrolysis time

Figure 5 demonstrates how the removal efficiency of the ion of Cu (II) ions with the help of iron–graphite electrodes was affected by the applied voltage (10 V, 30 V, and 50 V) over time. Removal efficiency increases with both an increase in voltage as well as time of electrolysis in Figure 5. The highest efficiency occurs continuously at 50 V, 30 V, and 10V. This is because of higher current densities at high voltages, which increase iron anode dissolution and coagulant (Fe^{2+}/Fe^{3+}) formation, and increased gas evolution, which promotes mixing and flotation. The Fe-graphite interface significantly improves electron transfer by providing a conductive pathway, which accelerates the Fe^{2+}/Fe^{3+} redox cycle. This enhancement boosts reaction kinetics, reduces energy loss, and increases the efficiency and stability of electrochemical processes involving iron electrodes. For Cu (II) shown in Figure 5, removal efficiency increases steadily up to where 50 V achieves almost complete removal in 10–15 minutes and is stable at 25 minutes. This is an indication of effective electrochemical reduction and co-precipitation with iron flocs [22], indicating the effect of voltage as well as system chemistry on electrocoagulation performance.

3.1.2 Removal efficiency at different electrode distances and electrolysis time

Figure 6 shows the effect of varying the electrode distances (2 cm, 3 cm, and 4 cm) on the removal efficiencies of Cu (II) ion with iron–graphite electrodes at constant voltage (50 V) over different electrolysis durations with regards to horizontal point of intersection. Regardless of Figure 6, 3 cm electrode spacing is found to be optimal in all cases, followed by 4 cm, and 2 cm gives the least removal efficiency. This trend emphasizes the significance of optimal spacing to successful electrochemical reaction. At 3 cm, the system probably maintains an equilibrium between electric field strength and ionic mobility for effective coagulant production, enhanced floc interaction, and maintenance of gas bubble dispersion. On the contrary, the 2 cm spacing might cause excessive gas evolution and localized turbulence or, even, short-circuiting, which will interfere with the floc formation. At 4 cm, greater clearance can reduce the current density and introduce higher resistance, degrading the efficiency of the overall process. In Figure 6, Cu (II) removal, there is steady growth in efficiency with time for all spacings, with 3 cm clearly outperforming the rest, being effective in high removal from 15–20 minutes. This result is an illustration of the advantages of well-dispersed coagulants and controlled gas evolution at appropriate spacing. The 3 cm distance provides an optimal balance for maximizing removal efficiency, supporting earlier studies such as study [23] on the influence of inter-electrode distance in such systems.

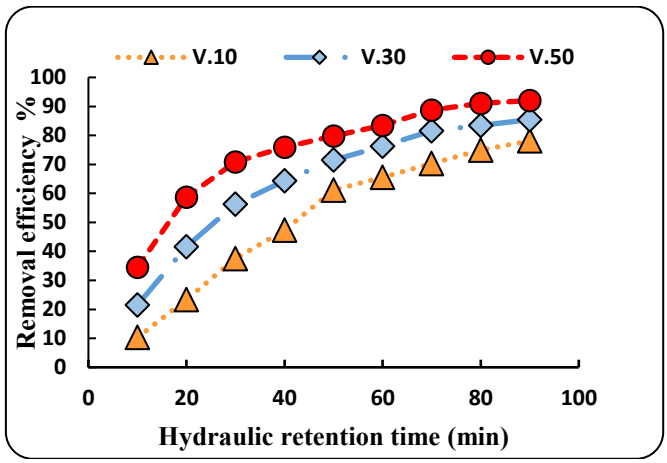

Figure 5. Effect of the different applied voltage and electrolysis time on removal efficiency of Cu (II) ion from (Iron + graphite) electrodes

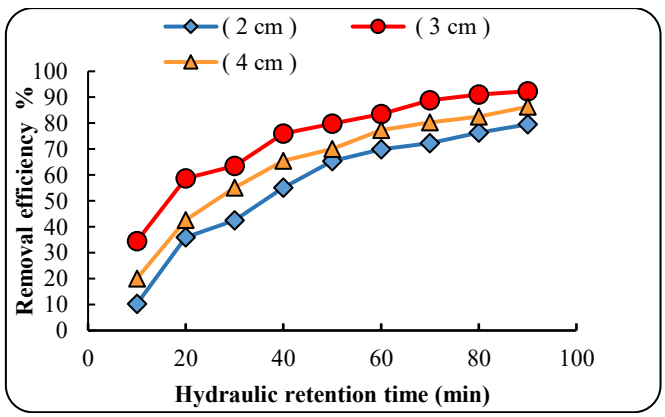

Figure 6. Effect of the different electrode distances, 50 V, and electrolyzation time on removal efficiency of Cu (II) ion from (Iron + graphite) electrodes

3.1.3 Removal efficiency at different other parameters

Figure 7 presents changes in key supporting parameters, electrical conductivity (EC), total dissolved solids (TDS), temperature, electric current, and pH during Cu (II) removal via electrocoagulation using iron–graphite electrodes at applied voltages of (a) 10 V, (b) 30 V, and (c) 50 V. At all voltage levels, both EC and TDS decreased over time, indicating the effective removal of dissolved ionic species

through coagulation and precipitation. The most significant reduction occurred at 50 V, reflecting enhanced ionic destabilization and metal removal at higher voltage. Temperature steadily increased across all conditions, with greater rises at higher voltages due to Joule heating. This heat generation may improve reaction rates and coagulant solubility, though excessive temperatures could risk floc destabilization if uncontrolled. Electric current showed a slight upward trend, especially at 50 V, likely due to ongoing electrode dissolution and reaction activity. The rise suggests sustained conductivity and an active electrochemical environment. pH remained relatively stable throughout the experiments, with only minor fluctuation. This stability may result from the water's buffering capacity and limited hydrogen or hydroxide ion production under the tested conditions. Maintaining a steady pH is beneficial, as significant shifts could impair metal hydroxide formation and reduce removal efficiency [24].

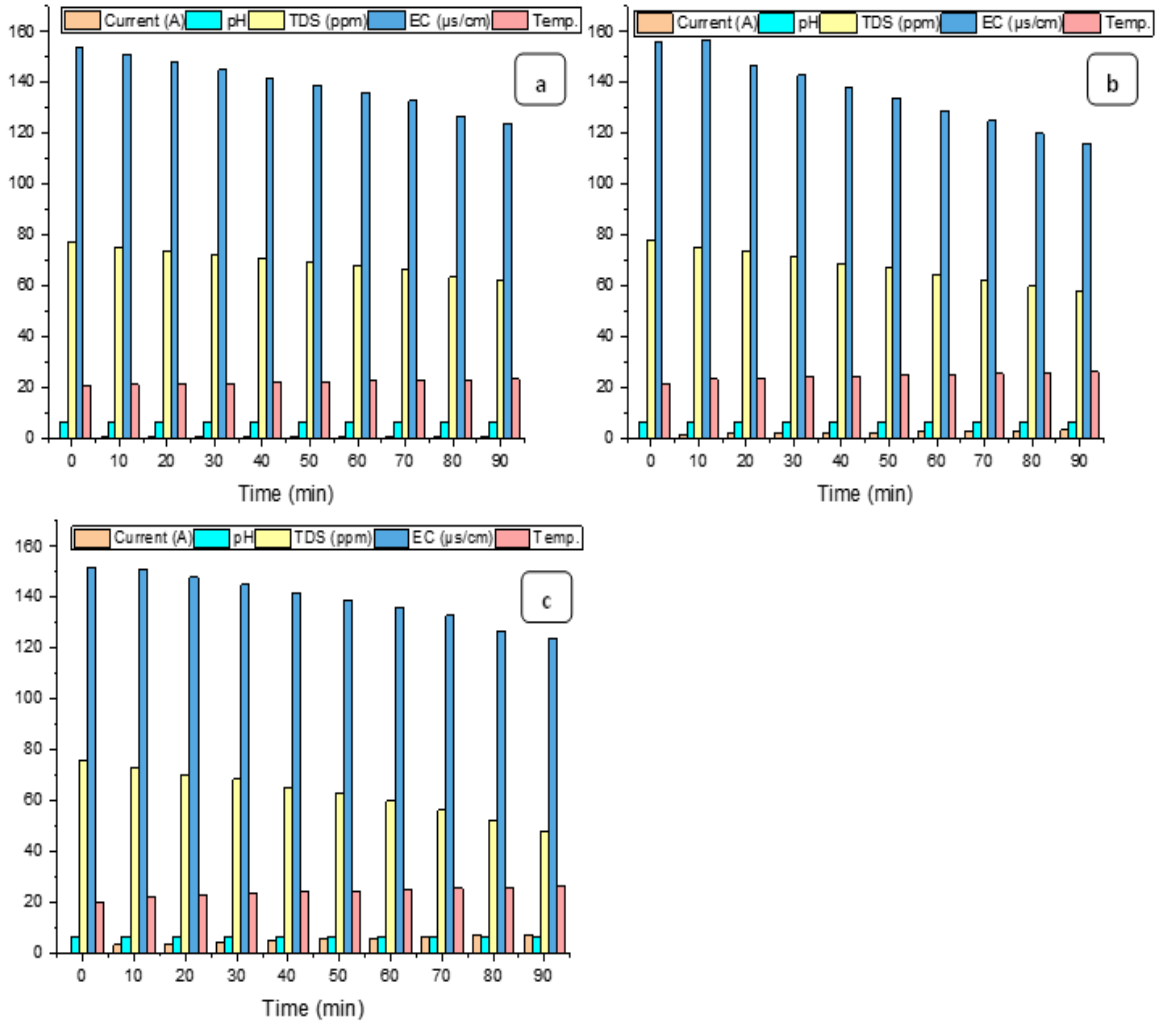

Figure 7. Effect of the different parameters and electrolysis time on removal efficiency of Cu (II). (a) 10 V, (b) 30 V, (c) 50 V from (Iron + graphite) electrodes

3.2 Continuous electrocoagulation results

3.2.1 Removal efficiency at different flow rates

In Figure 8, which illustrates the effect of 50 V applied voltage, 3 cm electrode distance, different flow rates, and electrolyzation time on the removal efficiency of Cu (II) ion, the results demonstrate that the 0.3 L/min flow rate achieved the highest removal efficiency, reaching approximately 90% for the contaminants. This flow rate was superior to the 0.2 L/min and 0.1 L/min flow rates at lower efficiencies of removal. The enhanced performance at a flow rate of 0.3 L/min is explained by the fact that it provides appropriate contact time with necessary flow for continuous processing. With such a flow rate, the water remains in contact with the electrodes long enough for them to reach the required coagulation and precipitation of the contaminants. The coagulation process, which is important to remove metal ions such as Cu (II), requires optimized conditions for the formation of stable flocs, which can be removed from the water. Under condition of a low flow rate (in the case of 0.1 L / min), the system undergoes a slow water movement through the reactor, resulting in an unacceptably long residence time. Although this may appear advantageous for prolonging the contact time, it might cause inefficiencies as this would not be a system that would be designed for a continuous flow, and therefore, the overall removal efficiency would drop. The same applies to a 0.2 L/min flow rate, which is marginally preferable, but does not offer the same ideal dynamic as the 0.3 L/min flow rate. At this intermediate rate, the flow is too slow, but still does not provide the maximum effective treatment observed at the higher flow rate. At 0.3 L/min flow rate, optimal removal of contaminants in the (Iron + Graphite) is achieved because of maximizing the contact time between contaminants and electrodes that still allows for continuous

flow [25]. Such balance brings up the most efficient removal; the removal rate reaches approximately 90% for metals under study.

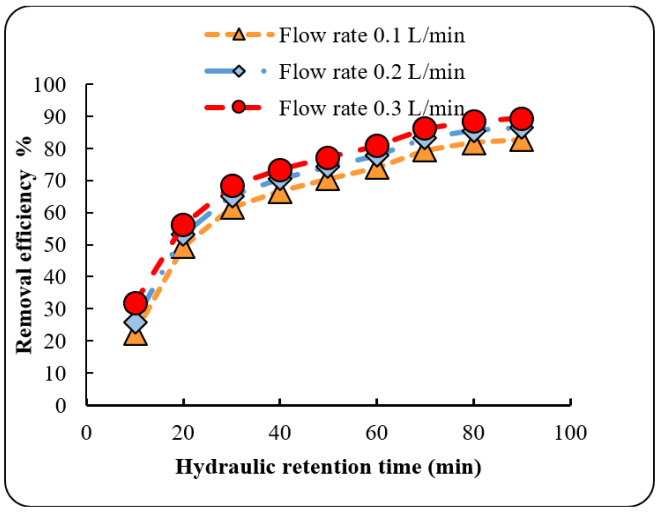

Figure 8. Effect of 50 V applied voltage, 3 cm electrode distance, different flow rate, and electrolyzation time on removal efficiency of Cu (II) ion from (Iron + graphite) electrodes

3.2.2 Removal efficiency at different other parameters

Figure 9 shows the experimental data that shows the effect of the operational variables flow rate and electrolysis time on the efficiency of removing Cu (II) using iron-graphite electrodes. Three flow rates were studied: (a) 0.1 L/min, (b) 0.2 L/min, and (c) 0.3 L/min. The results indicate that Cu (II) removal efficiency increases with an increase in flow rates. The removal efficiency was the lowest at a flow rate of 0.1 L/min. This finding is in line with the lack of contact time between electrodes and pollutants, resulting in low coagulation and precipitation. The low water velocity limited the effectiveness of the electrocoagulation process since Cu ions did not have adequate contact with coagulating agents, thus failing to form flocculated structures. An incremental increase was seen at 0.2 L/min; the increased flow rate resulted in better mixing of the solution, which improved contact between Cu ions and electrodes. However, the efficiency was not equal to the one obtained at 0.3 L/min, which means that the best results are achieved at flow rates higher than 0.2 L/min. The maximum removal efficiencies were obtained at the flow rate of 0.3 L/min, which is a trade-off between contact time and dynamic forces. At this speed, the solution spent sufficient time at the electrodes to allow coagulation, floc formation, and high metal-ion removal rates. Furthermore, the high flow rate provided an easy dispersion of hydrogen gas, better mixing, and flotation of flocs, which eventually increased the efficiency of Cu (II) removal [4, 26].

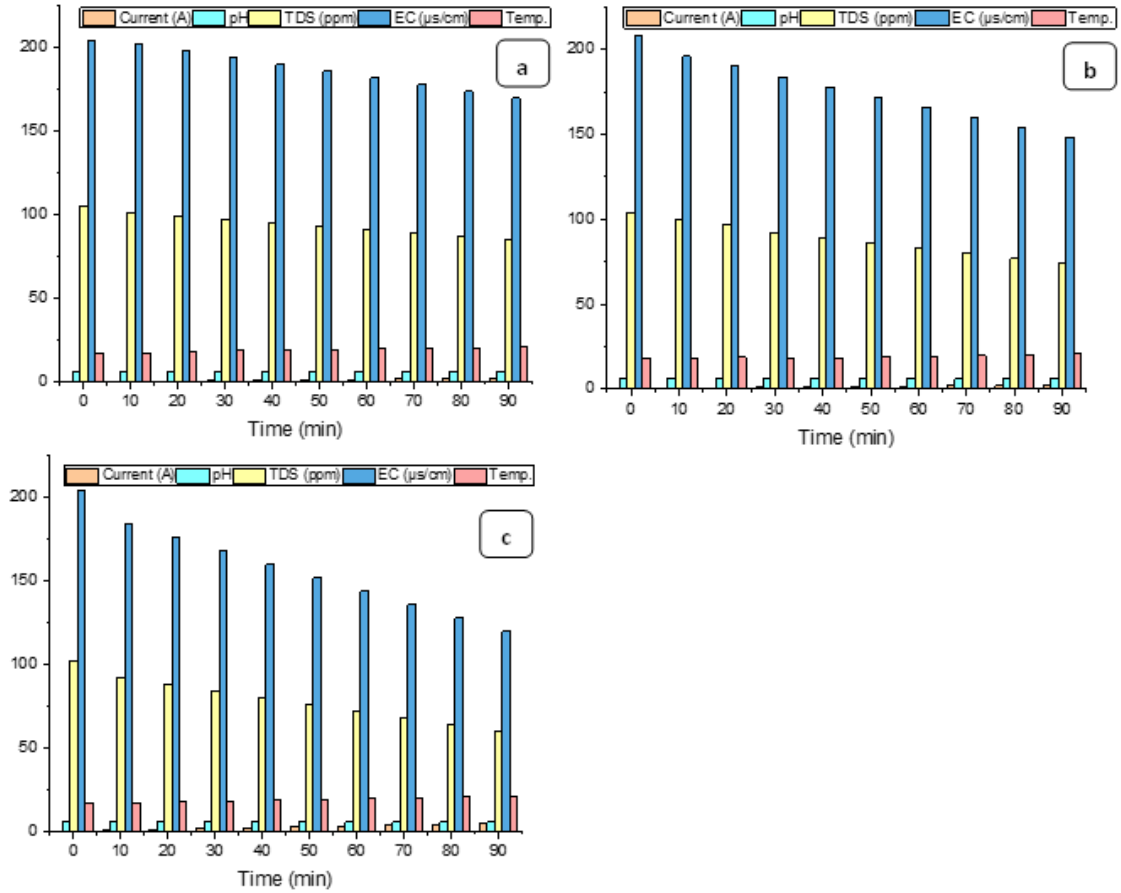

Figure 9. Effect of the different parameters and electrolysis time on removal efficiency of Cu (II). (a) Flow rate 0.1 L/min, (b) Flow rate 0.2 L/min, (c) Flow rate 0.3 L/min from (Iron + graphite) electrodes

3.2.3 Cost, revenue, and Energy generated by Hydrogen gas

Different experiments were carried out in order to study the conversion of the H_2 gas (L) to green Energy fuel (KW) and cost revenue ($) concerning the Flow rate (0.1, 0.2, 0.3) L/min, and the operating condition included 50 V applied voltage as shown in Figure 10.

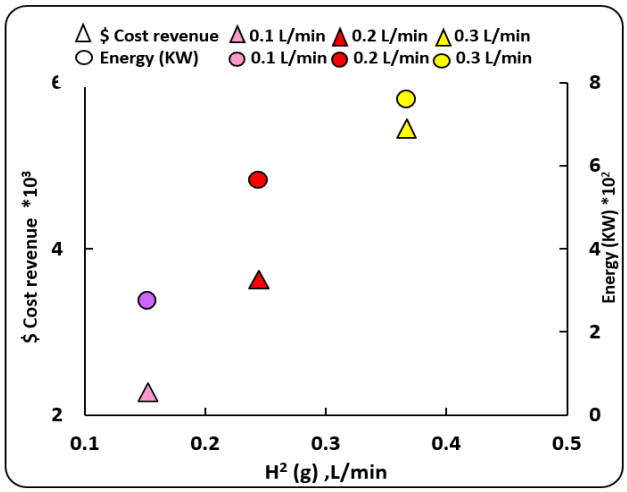

Figure 10. Cost, revenue, and Energy generated Hydrogen gas (L) at different flow rates from Cu (II) (Iron + graphite) electrodes

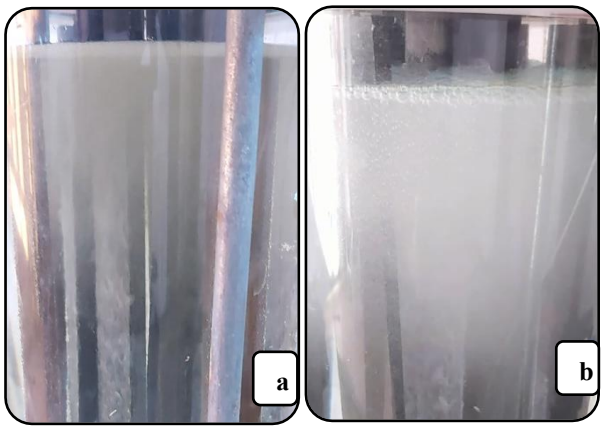

Figure 11. Hydrogen bubbles (a) Photographic diagram of continuous electrocoagulation instruments with iron anode and graphite cathode, (b) Photographic diagram of continuous electrocoagulation instruments with four iron anodes and four graphite cathodes

The hydrogen gas bubbles are generated as shown in Figure 11, and determine the hydrogen generated and convert it to energy and cost revenue by using it as a fuel. determine the TDS, EC, pH, and Temperature inside the reactor. During the experiment, the dissolution of ions occurred, and the generation of hydrogen gas was collected in a balloon as shown in Figure 12. The hydrogen production efficiency decreases as the residence time within the electrocoagulation reactor shortens. This reduction limits the duration for electrochemical reactions to occur, thereby lowering hydrogen generation, necessitating a trade-off between pollutant removal and energy output in Fe-graphite electrocoagulation.

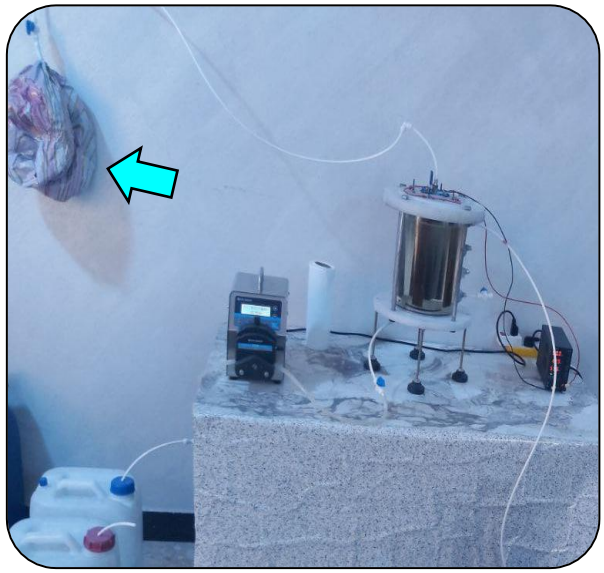

Figure 12. Hydrogen gas balloon collector during the experiments

3.3 Kinetics models in batch EC reactor

The study findings indicate that the pseudo-second-order model can be used to describe the diffusion-controlled process better than the pseudo-first-order model. As indicated in Figures 13(a) and (b), the R^2 of the pseudo-first-order and pseudo-second-order models were 0.86 and 0.98, respectively. This suggests that the process may be governed by surface chemical factors or complex molecular interactions that the pseudo-first-order model cannot accurately represent.

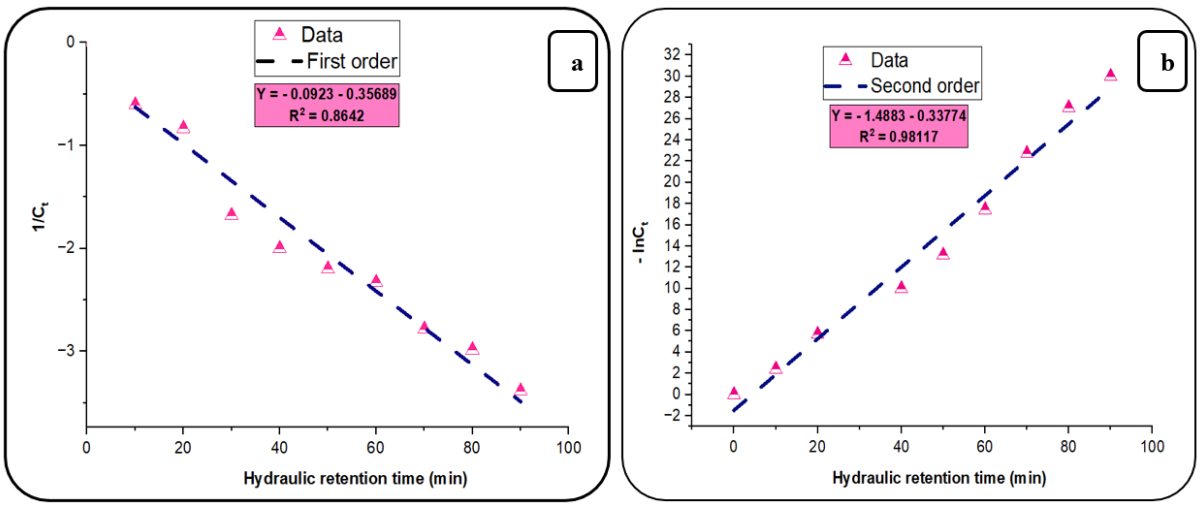

Figure 13. Plots of the first-order and second-order reaction models of the experimental data of the Cu (II) ion removal in a batch EC reactor (Experimental conditions: Temperature: 26.7°C; pH: 7; Electrode distance: 3 cm; Voltage: 50 V; Reaction time: 90 min)

4. CONCLUSIONS

This paper examined the effectiveness of electrocoagulation with Fe-Gr electrodes in the removal of Cu (II) in aqueous solutions. The results show that Fe-Gr electrodes significantly increase the efficiency of removal compared to the traditional techniques, which is explained by the synergetic effect of the coagulant effect of iron and the large surface area of graphite, which increases the adsorption capacity. The findings show that the operational parameters, namely, applied voltage, inter-electrode distance, and treatment time, have an important impact on the removal performance. The best conditions were obtained at an applied voltage of 50 V and an inter-electrode spacing of 3 cm the presence of graphite minimizes anode passivation by facilitating efficient electron transport and preserving surface conductivity, thereby enhancing overall electrochemical activity and system stability, where almost 100 percent Cu (II) removal was achieved in 25 min of batch treatment. Continuous operation gave a flow rate of 0.3 L/min which gave a 90% removal efficiency of Cu (II), which shows the significance of optimizing the flow-rate. The kinetic data indicate that the removal follows a pseudo-second-order model with an R^2 of 0.98, which highlights the fact that chemical sorption is the rate-limiting process. Other interesting results were the release of hydrogen gas in the electrolysis process. The hydrogen gas produced catholically can be harnessed as a green fuel thus making the process more sustainable. The produced hydrogen can be used to produce energy, which has both environmental and economic benefits. All these findings point to the fact that electrocoagulation with Fe-Gr electrodes is a potentially good wastewater treatment and energy recovery technology that can be used to address the problem of environmental contamination in a sustainable and cost-effective manner. The synthetic wastewater prepared for the experiment was designed to replicate the key physicochemical properties of real wastewater, allowing the test conditions to realistically simulate practical treatment environments and support accurate performance assessment.

ACKNOWLEDGMENT

The authors are thankful to the Department of Environmental Engineering, University of Baghdad for their support and offering the technical facilities required for experimental work.

REFERENCES

[1] Boulanouar, L., Louhichi, B., Hamdi, W., Jellali, S., L'taief, B., Hamdi, N., Rebouh, N.Y., Houas, A. (2025). Parametric study of cadmium and nickel removal from synthetic and actual industrial wastewater industry by electrocoagulation using solar energy. Journal of Water Process Engineering, 71: 107261. https://doi.org/10.1016/j.jwpe.2025.107261

[2] Bakry, S.A., Matta, M.E., Noureldin, A.M., Zaher, K. (2024). Performance evaluation of electrocoagulation process for removal of heavy metals from wastewater using aluminum electrodes under variable operating conditions. Desalination and Water Treatment, 318: 100396. https://doi.org/10.1016/j.dwt.2024.100396

[3] Hassan, G.S., Abbar, A.H. (2025). Electrocoagulation process for cobalt removal from industrial wastewater: Optimization and kinetic study. South African Journal of Chemical Engineering, 53: 233-241. https://doi.org/10.1016/j.sajce.2025.05.001

[4] Shahedi, A., Jamshidi-Zanjani, A., Darban, A.K., Homaee, M., Taghipour, F. (2025). Nickel, cyanide, zinc, and copper removal from the effluent using photo-electrocoagulation-oxidation. Journal of Hazardous Materials Advances, 17: 100550. https://doi.org/10.1016/j.hazadv.2024.100550

[5] Yan, R., Luo, D., Fu, C., Wang, Y., Zhang, H., Wu, P., Jiang, W. (2020). Harmless treatment and selective recovery of acidic Cu (II)-Cr (VI) hybrid wastewater via coupled photo-reduction and ion exchange. Separation and Purification Technology, 234: 116130. https://doi.org/10.1016/j.seppur.2019.116130

[6] Pavithra, S., Thandapani, G., Alkhamis, H.H., Alrefaei, A.F., Almutairi, M.H. (2021). Batch adsorption studies on surface tailored chitosan/orange peel hydrogel composite for the removal of Cr (VI) and Cu (II) ions from synthetic wastewater. Chemosphere, 271: 129415. https://doi.org/10.1016/j.chemosphere.2020.129415

[7] Lu, J., Fan, R., Wu, H., Zhang, W., Li, J., Zhang, X., Sun, H., Liu, D. (2022). Simultaneous removal of Cr (VI) and Cu (II) from acid wastewater by electrocoagulation using sacrificial metal anodes. Journal of Molecular Liquids, 359: 119276. https://doi.org/10.1016/j.molliq.2022.119276

[8] Theydan, S.K., Mohammed, W.T., Haque, S.M. (2024). Three-dimensional electrocoagulation process optimization employing response surface methodology that operated at batch recirculation mode for treatment refinery wastewaters. Iraqi Journal of Chemical and Petroleum Engineering, 25(1): 59-74. https://doi.org/10.31699/IJCPE.2024.1.6

[9] Salman, R.H. (2019). Removal of manganese ions (Mn2+) from a simulated wastewater by electrocoagulation/electroflotation technologies with stainless steel mesh electrodes: Process optimization based on Taguchi approach. Iraqi Journal of Chemical and Petroleum Engineering, 20(1): 39-48. https://doi.org/10.31699/IJCPE.2019.1.6

[10] Al-Nuaimi, A.S., Pak, K.S. (2016). Chromium (VI) removal from wastewater by electrocoagulation process using taguchi method: Batch experiments. Iraqi Journal of Chemical and Petroleum Engineering, 17(4): 95-103. https://doi.org/10.31699/IJCPE.2016.4.9

[11] Edition, F. (2011). Guidelines for drinking-water quality. WHO Chronicle, 38(4): 104-108.

[12] Abdel-Shafy, H.I., Morsy, R.M., Hewehy, M.A., Razek, T.M., Hamid, M.M. (2022). Treatment of industrial electroplating wastewater for metals removal via electrocoagulation continous flow reactors. Water Practice & Technology, 17(2): 555-566. https://doi.org/10.2166/wpt.2022.001

[13] Mohammed, O.N., Abdulhameed, H.M. (2025). Solar powered electrocoagulation system for groundwater remediation at Al-Raaed Station for irrigation purposes: Batch Mode. International Journal of Design & Nature and Ecodynamics, 20(3): 633-645. https://doi.org/10.18280/ijdne.200318

[14] Ebba, M., Asaithambi, P., Alemayehu, E. (2022). Development of electrocoagulation process for

wastewater treatment: optimization by response surface methodology. Heliyon, 8(5): e09383. https://doi.org/10.1016/j.heliyon.2022.e09383

[15] Ibrahim, D.T., Hameed, H.M.A. (2021). Study hybrid treatment technologies using (MBBR with Electro-flotation) for Textile wastewater. Journal of Physics: Conference Series, 2114(1): 012052. https://doi.org/10.1088/1742-6596/2114/1/012052

[16] Nidheesh, P.V., Singh, T.A. (2017). Arsenic removal by electrocoagulation process: Recent trends and removal mechanism. Chemosphere, 181: 418-432. https://doi.org/10.1016/j.chemosphere.2017.04.082

[17] Huang, Y., Li, S., Chen, J., Zhang, X., Chen, Y. (2014). Adsorption of Pb (II) on mesoporous activated carbons fabricated from water hyacinth using H_3PO_4 activation: Adsorption capacity, kinetic and isotherm studies. Applied Surface Science, 293: 160-168. https://doi.org/10.1016/j.apsusc.2013.12.123

[18] Al-Rubaie, Z.Y., H Faisal, A.A. (2025). Sorption of tetracycline from contaminated water using magnesium-iron layered double hydroxide alginate beads prepared from Schanginia aegyptica and scrap iron. Journal of Ecological Engineering, 26(4): 209-219. https://doi.org/10.12911/22998993/199820

[19] Ali, A.A., Abdul-Hameed, H.M. (2025). Synthesis and characterization of magnetic activated carbon manufactured from palm stones by physical activation to remove lead from aqueous solution. Desalination and Water Treatment, 321: 100951. https://doi.org/10.1016/j.dwt.2024.100951

[20] Ali, H.Q., Mohammed, A.A. (2020). Elimination of Congo red dyes from aqueous solution using Eichhornia crassipes. Iraqi Journal of Chemical and Petroleum Engineering, 21(4): 21-32. https://doi.org/10.31699/IJCPE.2020.4.3

[21] Kashi, G. (2023). Electrocoagulation/flotation process for removing copper from an aqueous environment. Scientific Reports, 13: 13334. https://doi.org/10.1038/s41598-023-40512-y

[22] Qiu, A., Qian, A., Liao, P., Xie, S. (2025). In-situ generation of diverse Fe (II) species via iron electrocoagulation for redox transformation of contaminants− A critical review. Separation and Purification Technology, 354: 129224. https://doi.org/10.1016/j.seppur.2024.129224

[23] Modirshahla, N., Behnajady, M.A., Kooshaiian, S. (2007). Investigation of the effect of different electrode connections on the removal efficiency of Tartrazine from aqueous solutions by electrocoagulation. Dyes and Pigments, 74(2): 249-257. https://doi.org/10.1016/j.dyepig.2006.02.006

[24] Weiss, S.F., Christensen, M.L., Jørgensen, M.K. (2021). Mechanisms behind pH changes during electrocoagulation. AIChE Journal, 67(11): e17384.

[25] Su, P., Song, G., Wang, X., Zhang, Q., Fu, W., Zhou, M. (2023). Novel self-sustained flow-through electrochemical advanced oxidation processes using nano-Fe^0 confined B, N co-doped carbon nanotubes/graphite felt cathode: Higher mineralization efficiency under wider pH. Separation and Purification Technology, 318: 123944. https://doi.org/10.1016/j.seppur.2023.123944

[26] Peng, W., Lv, S., Cao, Y., Wang, W., Liu, S., Huang, Y., Fan, G. (2023). A novel pH-responsive flocculant for efficient separation and recovery of Cu and Mo from secondary resources via selective flocculation-flotation. Journal of Cleaner Production, 395: 136463. https://doi.org/10.1016/j.jclepro.2023.136463